

Doubly hybrid density functional for accurate descriptions of nonbond interactions, thermochemistry, and thermochemical kinetics

Ying Zhang^a, Xin Xu^{a,1}, and William A. Goddard III^{b,1}

^aDepartment of Chemistry, State Key Laboratory of Physical Chemistry of Solid Surfaces, Center for Theoretical Chemistry, College for Chemistry and Chemical Engineering, Xiamen University, Xiamen 361005, China; and ^bMaterials and Process Simulation Center (139-74), California Institute of Technology, Pasadena, CA 91125

Contributed by William A. Goddard III, February 6, 2009 (sent for review November 25, 2008)

We develop and validate a density functional, XYG3, based on the adiabatic connection formalism and the Görling–Levy coupling-constant perturbation expansion to the second order (PT2). XYG3 is a doubly hybrid functional, containing 3 mixing parameters. It has a nonlocal orbital-dependent component in the exchange term (exact exchange) plus information about the unoccupied Kohn–Sham orbitals in the correlation part (PT2 double excitation). XYG3 is remarkably accurate for thermochemistry, reaction barrier heights, and nonbond interactions of main group molecules. In addition, the accuracy remains nearly constant with system size.

Becke 3-parameter hybrid functional combined with Lee–Yang–Parr correlation functional | density functional theory | generalized gradient approximation | local density approximation | mean absolute deviation

Density functional theory (DFT) has revolutionized the role of theory by providing accurate first-principles predictions of critical properties for applications in physics, chemistry, biology, and materials science (1). Despite dramatic successes, there remain serious deficiencies, for example, in describing weak interactions (London dispersion), which are so important to the packing of molecules into solids, the binding of drug molecules to proteins, and the magnitude of reaction barriers. We propose here a DFT functional that dramatically improves the accuracy for these properties by including the role of the virtual (unoccupied) states.

Solution of the Schrödinger equation leads to the wavefunction, $\psi(r_1, r_2, \dots, r_N)$ (2), which depends on the $3N$ space coordinates and N spin coordinates of N -electrons in the system. Solving for such a wavefunction usually starts with the Hartree–Fock (HF) mean field description involving N self-consistent 1-particle spin-orbitals (in a Slater determinant), which is then used as the basis for expanding the wavefunction in a hierarchy of excited N -electron configurations, by using methods referred to as Møller–Plesset theory (e.g., MP2, MP3, MP4), couple-cluster theory (e.g., CCSD(T)), and quadratic configuration interaction theory (e.g., QCISD(T)), etc. These methods are ab initio but suffer from problems of slow convergence with the size of the basis sets and the configuration expansion lengths, preventing scaling to large systems.

In contrast, DFT is formulated in terms of the 1-particle density, $\rho(r)$, depending on only 3 spatial coordinates rather than $3N$, as the fundamental quantity (3, 4). This dramatically simplifies the process of calculating the structures and properties. However, the exact form of the functional, whose solution will lead to the correct density, is not known. Even so, there has been an evolution of successively better approximations to this functional, that has already provided quite good accuracy for many problems (5–15).

Perdew (16) has formulated the hierarchy of DFT approximations as a “Jacob’s ladder” rising from the “earth of Hartree” to the “heaven of chemical accuracy.” The first rung of this ladder is the local (spin) density approximation [LDA, e.g.,

SVWN (4, 5)] and the second rung is the generalized gradient approximation [GGA, e.g., BLYP (6, 7) and PBE (8)]. Although LDA uses densities $\rho(r)$ as local ingredients, GGA employs both the local densities and their gradients $\nabla\rho(r)$. The third rung is termed metaGGA [e.g., TPSS (9)], which expands GGA to include further the kinetic energy density τ , and/or the Laplacian of the density $\nabla^2\rho(r)$. Up to this third rung, they are all local and multiplicative.

The fourth rung of DFT is a hybrid that introduces nonlocality by replacing some portion of the local exchange energy density with the exact (HF-like) exchange energy density. The most popular such hyperGGA flavor is B3LYP (5–7, 10), which has been shown to provide accurate predictions for thermochemistry of small covalent systems (11). However, B3LYP is poor for the predictions of noncovalent bonding interactions (15) and reaction barrier heights (14), with performance degrading dramatically as system sizes increase (12, 13).

The final fifth rung of Jacob’s ladder utilizes the unoccupied Kohn–Sham (KS) orbitals (16) in addition to the occupied KS orbitals. This final rung is expected to allow the heaven of chemical accuracy to be achieved for broad applications. However, no such functional based on first principles (17) and practical for general use has been proposed. Empirical versions (18) have led to promising results for thermochemistry and reaction barriers, but they still fail to account for van der Waals interactions.

Here, we develop a fifth-rung functional that incorporates information about the unoccupied KS orbitals [based on the Görling–Levy coupling-constant perturbation expansion to the second order (19)], along with 3 empirical mixing parameters. We demonstrate that this functional is highly accurate for thermochemistry, reaction barriers, and nonbond interactions.

Theory

DFT was placed on a firm theoretical footing by the Hohenberg–Kohn (HK) theorems (3). These HK theorems prove that there exists a total energy functional $E[\rho]$, from which one can obtain the ground state electron density ρ_0 by minimizing $E[\rho]$ with respect to the density ρ ,

$$E[\rho_0] = \text{Min}_{\rho} E[\rho]. \quad [1]$$

where ρ_0 contains all information that can be known about the electronic structure of the system. However, the HK theorems do not specify this true total energy functional.

Author contributions: X.X. and W.A.G. designed research; Y.Z. and X.X. performed research; Y.Z., X.X., and W.A.G. analyzed data; and Y.Z., X.X., and W.A.G. wrote the paper.

The authors declare no conflict of interest.

¹To whom correspondence may be addressed. E-mail: xinxu@xmu.edu.cn or wag@wag.caltech.edu.

This article contains supporting information online at www.pnas.org/cgi/content/full/0901093106/DCSupplemental.

The most popular implementation of DFT is through the KS method (4), which assumes a noninteracting N-electron system having the same density as the original many-body system. The KS wavefunction can be expressed exactly as a Slater determinant leading to an exact form for the kinetic energy T_s of the noninteracting system and the classic Coulomb energy U . The total energy is then expressed as

$$E = T_s + U + V_{\text{ext}} + E_{\text{xc}}, \quad [2]$$

where V_{ext} is the external potential energy, and E_{xc} is the exchange-correlation energy, which remains unknown.

The adiabatic connection formalism (10, 20–25) provides a rigorous way to define E_{xc} . It assumes an adiabatic path between the fictitious noninteracting KS system ($\lambda = 0$) and the physical system ($\lambda = 1$) while holding the electron density ρ fixed at its physical $\lambda = 1$ value for all λ of a family of partially interacting N-electron systems:

$$E_{\text{xc}}[\rho] = \int_0^1 U_{\text{xc},\lambda}[\rho] d\lambda. \quad [3]$$

$U_{\text{xc},\lambda}$ is the potential energy of exchange correlation at intermediate coupling strength λ . The only problem is that the exact integrand $U_{\text{xc},\lambda}$ is unknown.

Becke first used this formalism as a practical tool for functional construction (10, 23) by assuming a linear model (23)

$$U_{\text{xc},\lambda} = a + b\lambda, \quad [4]$$

and taking $U_{\text{xc},\lambda=0} = E_x^{\text{exact}}$, the exact exchange of the KS orbitals, and approximating $U_{\text{xc},\lambda=0} \approx U_{\text{xc},\lambda=0}^{\text{LDA}}$. Becke's half-and-half functional (23) may be approximated by

$$E_{\text{xc}}[\rho] = \frac{1}{2} (E_x^{\text{exact}} + E_x^{\text{LDA}}) + \frac{1}{2} E_c^{\text{LDA}}, \quad [5]$$

where we have partitioned $E_{\text{xc}}^{\text{LDA}} = E_x^{\text{LDA}} + E_c^{\text{LDA}}$ and set

$$a = E_x^{\text{exact}}, \quad b = E_{\text{xc}}^{\text{LDA}} - E_x^{\text{exact}}. \quad [6]$$

The popular Becke's 3-parameter functional modifies Eq. 5 empirically to obtain Eq. 7 (10):

$$E_{\text{xc}}^{\text{B3}}[\rho] = E_{\text{xc}}^{\text{LDA}} + c_1(E_x^{\text{exact}} - E_x^{\text{LDA}}) + c_2\Delta E_x^{\text{GGA}} + c_3\Delta E_c^{\text{GGA}}, \quad [7]$$

where ΔE_x^{GGA} is the gradient-containing correction terms to the LDA exchange and ΔE_c^{GGA} is the gradient-containing correction to the LDA correlation, whereas $\{c_1, c_2, c_3\}$ are constants fitted against selected experimental thermochemical data. The success of Eq. 7 in achieving high accuracy demonstrates that errors of $E_{\text{xc}}^{\text{DFT}}$ for covalent bonding arise principally from the $\lambda \rightarrow 0$ or exchange limit, making it important to introduce some portion of exact exchange (10, 23–25).

An alternative to fixing the $\{a, b\}$ parameters in Eq. 4 is to use the Görling–Levy theory of coupling-constant perturbation expansion (19), in which the initial slope ($U'_{\text{xc},\lambda=0}$) is defined by the second-order correlation energy:

$$U'_{\text{xc},\lambda=0} = \left. \frac{\partial U_{\text{xc},\lambda}}{\partial \lambda} \right|_{\lambda=0} = 2E_c^{\text{GL2}}. \quad [8]$$

We may define E_c^{GL2} as (19):

$$E_c^{\text{GL2}} = -\frac{1}{4} \sum_{ij} \sum_{\alpha\beta} \frac{|\langle \varphi_i \varphi_j | \hat{v}_{\text{ee}} | \varphi_\alpha \varphi_\beta \rangle|^2}{\varepsilon_i + \varepsilon_j - \varepsilon_\alpha - \varepsilon_\beta} + \sum_i \sum_\alpha \frac{|\langle \varphi_i | \hat{v}_x - \hat{f} | \varphi_\alpha \rangle|^2}{\varepsilon_i - \varepsilon_\alpha}, \quad [9]$$

where \hat{v}_{ee} is the electron–electron repulsion operator, \hat{v}_x is the local exchange operator, and \hat{f} is the Fock-like, nonlocal exchange operator. We may calculate E_c^{GL2} from the KS orbitals with eigenvalues ε , where the subscripts (i, j) and (α, β) denote the occupied and unoccupied KS orbitals, respectively.

Combining Eq. 8 with Eq. 4 leads to:

$$b = 2E_c^{\text{GL2}}. \quad [10]$$

Eqs. 6 and 10 lead to 2 choices of b , which we combine using empirical parameters, $\{b_1, b_2\}$, to optimize the functional performance:

$$b = b_1 E_c^{\text{GL2}} + b_2 (E_{\text{xc}}^{\text{DFT}} - E_x^{\text{exact}}). \quad [11]$$

In principle, $E_c^{\text{DFT}} \approx (E_{\text{xc}}^{\text{DFT}} - E_x^{\text{exact}})$ contains a complete description of correlation effects, so that the second term of Eq. 11 may be interpreted as a way to extrapolate the second-order perturbation to infinite order. Hence, we propose to use an empirical formula of the form:

$$E_{\text{xc}}^{\text{R5}}[\rho] = E_{\text{xc}}^{\text{LDA}} + c_1(E_x^{\text{exact}} - E_x^{\text{LDA}}) + c_2\Delta E_x^{\text{GGA}} + c_3(E_c^{\text{PT2}} - E_c^{\text{LDA}}) + c_4\Delta E_c^{\text{GGA}}. \quad [12]$$

In comparison with the Becke 3-parameter scheme (10) of Eq. 7, Eq. 12 is a doubly hybrid DFT that mixes some exact exchange into E_x^{DFT} while also introducing a certain portion of E_c^{PT2} into E_c^{DFT} . Here, E_c^{PT2} contains the double-excitation contributions of E_c^{GL2} (i.e., the first term in Eq. 9). The single-excitation contributions in E_c^{GL2} may not be zero, but we absorb them into E_c^{DFT} and in the fitting parameters. Eq. 12 presents a fifth-rung functional (R5) that embodies information from both the occupied and the unoccupied KS orbitals as shown in Eq. 9.

In our current applications to test this functional, we calculate the B3LYP wavefunction and use the B3LYP orbitals as the KS orbitals to generate the density and to evaluate the PT2 term. Instead, the original GL2 perturbation theory (19) uses KS orbitals generated from a local exchange–correlation potential (see Eq. 9). Ref. 26 has shown that B3LYP densities are similar to those from CCSD(T) ab initio wavefunctions (for the molecules discussed in ref. 26). Nevertheless, the eigenvalues from B3LYP, whose potential is nonlocal, might differ considerably from those of the KS orbitals obtained from a local potential. Thus, it could be better to use some different set of KS orbitals.

Here, we adopt the LYP correlation functional but constrain $c_4 = (1 - c_3)$ in Eq. 12. This constraint is not necessary, but it eliminates 1 fitting parameter while excluding compensation from the LDA correlation term. The final 3 parameters $\{c_1, c_2, c_3\}$ are determined empirically by fitting only to thermochemical data of the G3/99 set, leading to:

$$\{c_1 = 0.8033, \quad c_2 = 0.2107, \quad c_3 = 0.3211\}. \quad [13]$$

We denote this generalized 3-parameter functional as XYG3.

Results and Discussion

Heats of Formation (Thermochemistry). The Gn paradigm developed by Pople and coworkers provides a hierarchy for extrapolating levels of correlation and basis sets to obtain increasingly accurate thermochemistry (11, 12, 27). To adjust the empirical

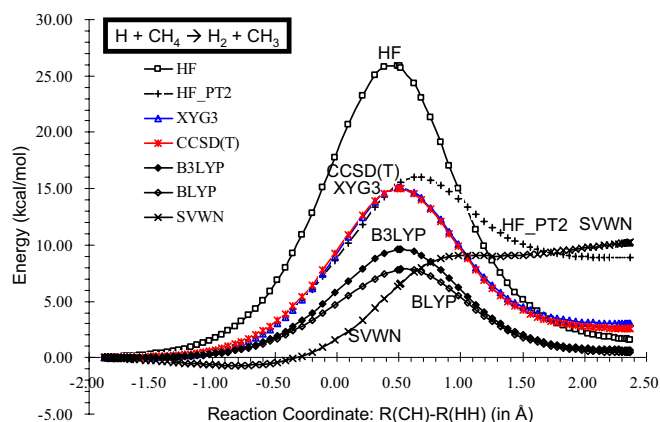


Fig. 1. Accuracy of various QM methods for calculating the potential energy surface for the $\text{H} + \text{CH}_4 \rightarrow \text{H}_2 + \text{CH}_3$ reaction coordinate [defined as $R(\text{CH}) - R(\text{HH})$]. The CCSD(T) calculations using the 6-311+G(3df,2pd) basis set, are expected to be the most accurate. B3LYP calculations were performed self-consistently by using the 6-311+G(3df,2p) basis set. All other results (HF, HF-PT2, XYG3, BLYP, and SVWN) used the density and orbitals from the B3LYP calculation. The XYG3 results superimpose nearly exactly on the CCSD(T) curve.

comparable with that of the QCISD(T) ab initio method with the same basis set (1.10 kcal/mol). We emphasize that barrier heights are not included in the XYG3 training set but are included in the M06 training set. Probably it is the presence of $\approx 80\%$ exact exchange in XYG3 that decreases the self-interaction errors (SIE) of local DFT functionals (25), whereas SIE make local DFT functionals problematic for the stretched partially broken bonds, characteristic of the transition states for chemical reactions.

Accurate potential energy surfaces (PES) are essential for using theory to predict chemical processes, but the accuracy depends critically on the level of the theory. Here, we test various methods for describing the $\text{H} + \text{CH}_4 \rightarrow \text{H}_2 + \text{CH}_3$ reaction. Because of its important roles in CH_4/O_2 combustion chemistry, this reaction has long been the subject of both experimental and theoretical interest (34). Fig. 1 presents a point-to-point comparison among the results of various methods along the reaction coordinate. We expect that the CCSD(T) curve should be the most accurate, leading to a barrier of 15.03 kcal/mol. Remarkably, XYG3 predicts the barrier of 15.08 kcal/mol, and is within 0.6 kcal/mol of the CCSD(T) results for the entire reaction path.

The LDA (SVWN) reaction path is qualitatively wrong, predicting a barrierless reverse reaction. HF overestimates the barrier height by 10.89 kcal/mol, whereas HF-PT2, which uses exact exchange plus PT2 correlation, overestimates the endothermicity of the reaction by 6.30 kcal/mol. Here, the tendency that BLYP underestimates the barrier heights is seen clearly in Fig. 1, whereas B3LYP, with inclusion of some exact exchange, leads to improved results, but remains inadequate for PES calculations.

Noncovalent Interactions. The noncovalent interaction DB from Zhao and Truhlar (14, 15) (NCIE31/05) consists of 6 HB complexes, 7 charge-transfer (CT) complexes, 6 dipole interaction (DI) complexes, 7 weak interaction (WI) complexes, and 5 π - π stacking (PPS) complexes. We tested the performance of the XYG3 functional for these noncovalent interactions using the 6-311+G(3df,2p) basis set, with geometries and reference energies taken from the Truhlar DB web site (14, 15).

The errors are summarized in Table 3. We did not include basis set superposition error corrections, which may increase the calculated interaction energies slightly.

Table 3. Accuracy of various QM methods for predicting noncovalent interactions

Functional	Total	HB6/04	CT7/04	DI6/04	WI7/05	PPS5/05
DFT						
M06-2X*	0.30	0.45	0.36	0.25	0.17	0.26
XYG3 [†]	0.32	0.38	0.64	0.19	0.12	0.25
M06*	0.43	0.26	1.11	0.26	0.20	0.21
M06-L*	0.58	0.21	1.80	0.32	0.19	0.17
B2PLYP [†]	0.75	0.35	0.75	0.30	0.12	2.68
B3LYP [†]	0.97	0.60	0.71	0.78	0.31	2.95
PBE [‡]	1.17	0.45	2.95	0.46	0.13	1.86
BLYP [‡]	1.48	1.18	1.67	1.00	0.45	3.58
LDA [‡]	3.12	4.64	6.78	2.93	0.30	0.35
Ab initio						
HF [†]	2.08	2.25	3.61	2.17	0.29	2.11
MP2 [‡]	0.64	0.99	0.47	0.29	0.08	1.69
QCISD(T) [‡]	0.57	0.90	0.62	0.47	0.07	0.95

MADs in kcal/mol for the 31 cases in the Truhlar web site DB (14, 15), which contains the best available information from ab initio calculations of noncovalent interactions (NCIE31/05). This consists of 6 HB complexes, 7 CT complexes, 6 DI complexes, 7 WI complexes, and 5 PPS complexes. The WI and PPS are dominated by London dispersion.

*Data are from ref. 14.

[†]Our calculations used the 6-311+G(3df,2p) basis sets with geometries from the Truhlar DB web site. Counterpoise corrections for possible basis set superposition errors were not included.

[‡]Data are from ref. 15.

We expect that the QCISD(T) ab initio method provides the highest accuracy, leading to a MAD = 0.57 kcal/mol. Remarkably M06-2X (MAD = 0.30) and XYG3 (MAD = 0.32) have half this error including WI and PPS for which London dispersion dominates. Also M06 (MAD = 0.43) and M06-L (MAD = 0.58) perform well for all 5 sets. Note that these nonbond interactions were not included in the XYG3 training set but were included in the M06 training set.

WI and PPS lead to notorious failures for common DFT methods because dispersion interactions are lacking in the correlation functionals. The PT2 term in XYG3 reduces this error, but B2PLYP was not able to describe the PPS complexes. It was suggested that this might be because the PT portion ($\approx 27\%$) is too small to overcome the repulsion from the DFT part (35). However, we suspect that it is because the orbitals from the truncated DFT in B2PLYP stray too far from the real KS orbitals.

Fig. 2 compares the intermolecular potentials of the CH_4 - C_6H_6 complexes calculated by XYG3 and CCSD(T) (36), along with some other DFT results. Proper description of such potential energy curves is very important for describing the binding of ligands to biological systems, because steric constraints might prevent the ligand from adopting its optimum geometry. We find that XYG3 results compare extremely well with those of CCSD(T), with deviations generally < 0.1 kcal/mol.

Fig. 2B shows the exchange contributions to the noncovalent interaction energy. Here, we see that XYG3 agrees closely with HF, which we expect to be the most accurate. We note here that Slater exchange (S) leads to a spurious well, whereas the GGA correction (Becke88) causes the potential curve to be far too repulsive.

Fig. 2C shows that correlation (attractive) contributions to the noncovalent interaction energy. Here, we see that XYG3 agrees closely with CCSD(T), which we expect to be the most accurate. Note that PT2 by itself is too attractive. Thus, it is the combination of PT2 with LYP that provides the excellent correlation description in XYG3.

That the exchange and correlation parts of XYG3 indepen-

27. Curtiss LA, Raghavachari K, Trucks GW, Pople JA (1991) Gaussian-2 theory for molecular energies of first- and second-row compounds. *J Chem Phys* 94:7221–7230.
28. Staroverov VN, Scuseria GE, Tao J, Perdew JP (2003) Comparative assessment of a new nonempirical density functional: Molecules and hydrogen-bonded complexes. *J Chem Phys* 119:12129–12137.
29. Wu JM, Xu X (2007) The X1 method for accurate and efficient prediction of heats of formation. *J Chem Phys* 127:214105–214113.
30. Zhao Y, Truhlar DG (2006) A new local density functional for main-group thermochemistry, transition metal bonding, thermochemical kinetics, and noncovalent interactions. *J Chem Phys* 125:194101–1–17.
31. Schwabe T, Grimme S (2006) Towards chemical accuracy for the thermodynamics of large molecules: New hybrid density functionals including non-local correlation effect. *Phys Chem Chem Phys* 8:4398–4401.
32. Kümmel S, Kronik L (2008) Orbital-dependent density functionals: Theory and applications. *Rev Mod Phys* 80:3–59.
33. Zhao Y, González-García N, Truhlar DG (2005) Benchmark database of barrier heights for heavy atom transfer, nucleophilic substitution, association, and unimolecular reactions and its use to test theoretical methods. *J Phys Chem A* 109:2012–2018.
34. Zhang LL, Lu YP, Lee S-Y, Zhang DH (2007) A transition state wave packet study of the H+CH₄ reaction. *J Chem Phys* 127:234313–1–7.
35. Schwabe T, Grimme S (2007) Double-hybrid density functionals with long-range dispersion corrections: Higher accuracy and extended applicability. *Phys Chem Chem Phys* 9:3397–3406.
36. Takatani T, Sherrill CD (2007) Performance of spin-component-scaled Møller–Plesset theory (SCS-MP2) for potential energy curves of noncovalent interactions. *Phys Chem Chem Phys* 9:6106–6114.
37. Kobayashi M, Imamura Y, Nakai H (2007) Alternative linear-scaling methodology for the second-order Møller–Plesset perturbation calculation based on the divide-and-conquer method. *J Chem Phys* 127: 074103–1–8.
38. Häser M, Almlöf J (1992) Laplace transform techniques in Møller–Plesset perturbation theory. *J Chem Phys* 96:489–494.
39. Rauhut G, Pulay P (1996) Considerations regarding the local treatment of Laplace transform MPPT. *Chem Phys Lett* 248:223–227.